



**HAL**  
open science

# Topological Pressure-Temperature State Diagram of the Crystalline Dimorphism of 2,4,6-trinitrotoluene

R. Céolin, Ivo B. Rietveld

► **To cite this version:**

R. Céolin, Ivo B. Rietveld. Topological Pressure-Temperature State Diagram of the Crystalline Dimorphism of 2,4,6-trinitrotoluene. *Fluid Phase Equilibria*, 2019, 506, pp.112395. 10.1016/j.fluid.2019.112395 . hal-02351479

**HAL Id: hal-02351479**

**<https://normandie-univ.hal.science/hal-02351479>**

Submitted on 6 Nov 2019

**HAL** is a multi-disciplinary open access archive for the deposit and dissemination of scientific research documents, whether they are published or not. The documents may come from teaching and research institutions in France or abroad, or from public or private research centers.

L'archive ouverte pluridisciplinaire **HAL**, est destinée au dépôt et à la diffusion de documents scientifiques de niveau recherche, publiés ou non, émanant des établissements d'enseignement et de recherche français ou étrangers, des laboratoires publics ou privés.

---

# TOPOLOGICAL PRESSURE-TEMPERATURE STATE DIAGRAM OF THE CRYSTALLINE DIMORPHISM OF 2,4,6-TRINITROTOLUENE

R. Céolin<sup>1</sup>, I. B. Rietveld<sup>2,3,\*</sup>

<sup>1</sup> LETIAM, EA7357, IUT Orsay, Université Paris Saclay, rue Noetzlin, 91405 Orsay, France

<sup>2</sup> Laboratoire SMS-EA3233, Université de Rouen Normandie, F76821, Mont Saint Aignan, France

<sup>3</sup> Faculté de Pharmacie, Université Paris Descartes, 4 avenue de l'observatoire, 75006 Paris, France

\* corresponding author: ivo.rietveld@univ-rouen.fr

## ABSTRACT

The phase behavior of explosive substances is important for the proper design of stable explosive devices. However, the equilibrium behavior of chemical compounds can be difficult to assess, because thermodynamic and kinetic behaviors are generally convoluted in the experimental results. The phase behavior of TNT is a case in point. A thorough review of the literature data demonstrates that the orthorhombic polymorph is the most stable under ambient conditions. Using the topological approach for the construction of a pressure-temperature phase diagram, it can be shown that all data is consistent with an overall enantiotropic system. Nonetheless, it is also clear that the differences between the orthorhombic and the monoclinic polymorphs are relatively small and that the driving force of interconversion between the two under ambient conditions is therefore limited.

Keywords: TNT, thermodynamics, phase behavior, phase diagram

# 1 INTRODUCTION

2,4,6-trinitrotoluene or TNT ( $C_7H_5N_3O_6$ ,  $M = 227.13 \text{ g mol}^{-1}$ ) possesses two crystalline polymorphs that can be obtained by slow evaporation at room temperature; one form is monoclinic and the other orthorhombic. According to Vrcelj et al. in 2003, the orthorhombic form is metastable and converts to the stable monoclinic form [1, 2]. Bowden et al. added to this in 2014: “*the orthorhombic phase is metastable at ambient pressure/temperature and was observed at high pressure*” [3], while referring to Stevens et al, who in fact had mentioned: “*the high pressure-temperature(P-T) stability of TNT has not been investigated in detail*” [4].

Considering the foregoing information, TNT appears to be an easy case for the construction of a topological pressure-temperature phase diagram to confirm the phase behavior and stability ranking of the two polymorphs found in the literature. The construction will be carried out in this paper.

## 2 AVAILABLE DATA ON TNT PHASE BEHAVIOR IN THE LITERATURE

### 2.1 CRYSTALLINE POLYMORPHISM

In the literature three polymorphs of TNT have been described of which two have been confirmed by crystal structure resolution. These are a monoclinic phase, form M, considered to be the more stable phase and an orthorhombic phase, form O. TNT melts at about  $81^\circ\text{C}$ .

#### 2.1.1 CRYSTALLOGRAPHIC DATA

In 1936, Hultgren reported values for room-temperature lattice parameters for the orthorhombic phase leading to a density of  $1.726 \text{ g cm}^{-3}$  with  $Z = 16$  molecules per unit-cell (see Table 1) [5]. This may have been reproduced by Winchell, as in his compilation, it is written that TNT is orthorhombic with a melting temperature of  $81^\circ\text{C}$  [6]. In 1982, Carper et al. reported the crystal and molecular structure of orthorhombic TNT at  $23^\circ\text{C}$ , space group  $Pca2_1$ ,  $V = 1823.6 \text{ \AA}^3$ , and  $Z = 8$  (Table 1) [7]. This leads to a density of  $1.655 \text{ g cm}^{-3}$ , which is considerably lower than that of the structure of Hultgren. In 1994, Golovina et al. obtained three kinds of crystals and two of those led to structures solved at room temperature [8]. The first one has an orthorhombic system, space group  $P2_1ca$ ,  $V = 1830.41 \text{ \AA}^3$ ,  $Z = 8$  and  $d = 1.6485 \text{ g cm}^{-3}$ , which is clearly similar to the structure found by Carper et al. (Table 1). The second form crystallizes in a monoclinic system, space group  $P2_1/b$ , with  $V = 1828.92 \text{ \AA}^3$ ,  $Z = 8$  and  $d = 1.650 \text{ g cm}^{-3}$ . A final form was found to be orthorhombic with a volume of  $3627 \text{ \AA}^3$  (Table 1), however, the structure has not been solved. This latter form resembles the one initially found by Hultgren. In 1996, Gallagher et al. reported that the crystal structures of the monoclinic and orthorhombic phases had been solved previously by Duke, who could not publish the results, because they had been classified [9]. The authors provided the lattice parameters of the two structures communicated by Duke in 1981 [9]: monoclinic  $P2_1/c$ , with  $V = 1827.52 \text{ \AA}^3$  and  $Z = 8$  leading to  $d = 1.6511 \text{ g cm}^{-3}$  and the orthorhombic form  $Pb2_1a$  with  $V = 1843.47 \text{ \AA}^3$  and  $Z = 8$  giving rise to  $d = 1.6368 \text{ g cm}^{-3}$ . In the following years Gallagher et al. produces more studies on the crystallization behavior of TNT and they come to the conclusion that even if the monoclinic form contains the lowest internal energy following lattice energy calculations, twinning of the monoclinic crystal tends to occur to a great extent and is only slightly more energetically unfavorable. The form highest in lattice energy according to the calculations is the orthorhombic form [9-11].

In 2003, Vrcelj et al. reexamined the structures of the two polymorphs at 100 and 123 K [2]. The monoclinic form,  $P2_1/a$ , was found to possess a volume of  $1761.37 \text{ \AA}^3$  leading to a density of  $1.713 \text{ g cm}^{-3}$  at 100 K. The orthorhombic form,  $Pca2_1$ , has a volume of  $V = 1770.58 \text{ \AA}^3$  and a density of  $1.704 \text{ g cm}^{-3}$  at 123 K. They also determined the expansivities of the two phases between 123 and 300K and found  $\alpha_M = 2.04 \times 10^{-4} \text{ K}^{-1}$  for the monoclinic phase and  $\alpha_0 = 1.95 \times 10^{-4} \text{ K}^{-1}$  for the orthorhombic one [1, 2]. These expansivities are very close to the mean value of  $2.21 \times 10^{-4} \text{ K}^{-1}$  found for solids made up of small molecules [12-14].

**Table 1. Crystallographic data on 2,4,6-trinitrotoluene in the literature and in the CSD**

Lattice system	<i>T</i> /K	<i>a</i> /Å	<i>b</i> /Å	<i>c</i> /Å	$\beta$ /°	<i>V</i> /Å <sup>3</sup>	<i>Z</i>	<i>d</i> /g cm <sup>-3</sup>	Ref <sup>a</sup>
Orthorhombic	RT	14.85	39.5	5.96	90	3496	16	1.726	[5] ZZZMUC03
Orthorhombic	RT	40.0	14.89	6.09	90	3627	16?	1.66?	[8] ZZZMUC07
Orthorhombic <i>P2<sub>1</sub>ca</i>	296	14.991(1)	6.077(1)	20.017(2)	90	1823.6	8	1.655	[7] ZZZMUC01
Orthorhombic <i>P2<sub>1</sub>ab</i>	RT	20.041(20)	15.013(8)	6.0836(5)	90	1830.41	8	1.648	[8] ZZZMUC05
Orthorhombic <i>Pb2<sub>1</sub>a</i>	RT?	15.075	20.024	6.107	90	1843.5	8	1.637	[9]
Orthorhombic <i>Pca2<sub>1</sub></i>	123	14.910(2)	6.034(18)	19.690(4)	90	1770.58	8	1.704	[2] ZZZMUC09
Monoclinic <i>P2<sub>1</sub>/b</i>	RT	21.407(20)	15.019(8)	6.0932(5)	111.005(20) ( $\gamma$ )	1828.86	8	1.650	[8] ZZZMUC06
Monoclinic <i>P2<sub>1</sub>/c</i>	RT?	21.275	6.093	15.025	110.23	1827.5	8	1.651	[9]
Monoclinic <i>P2<sub>1</sub>/a</i>	100	14.9113(1)	6.0340(1)	20.8815(3)	110.365(1)	1761.37	8	1.713	[2] ZZZMUC08
Monoclinic <i>P2<sub>1</sub>/*</i>	RT	20.2	6.2	7.7	90.0	964.3	4	1.56	[15] ZZZMUC
Monoclinic <i>C2/c</i>	RT	40.5	6.19	15.2	90.52	3810.4	16	1.58	[16] ZZZMUC02
Monoclinic <i>P2<sub>1</sub>/c</i>	RT	21.230(5)	6.081(2)	14.958(5)	110.12(2)	1813.23	8	1.664	[17] ZZZMUC04

<sup>a</sup> Literature reference and refcode of the Cambridge Structural Database (CSD)

### 2.1.2 CALORIMETRIC DATA

Already in 1969 it had been shown that an orthorhombic TNT polymorph on heating transforms endothermically to a monoclinic form before melting [18]. The enthalpy associated to this transition was found to be 0.27 kcal mol<sup>-1</sup> (1.13 kJ mol<sup>-1</sup>; 4.97 J g<sup>-1</sup>)[18]. Furthermore, the authors reported three different sequences of thermal behavior reflected in the DSC curves (Figure 1 and Table 2). The onset of the orthorhombic to monoclinic transition was observed in the temperature range of 63-64°C (336-337 K, peak a in Figure 1), whereas the onset temperature of the fusion of the monoclinic polymorph was found in the range of 78-80°C (351 – 353 K, peak b in Figure 1) [18]. Specimens “Q1” and “Q2”, which resulted in different thermal behavior (left-hand panel and center panel in Figure 1) possessed virtually the same X-ray diffraction pattern as the orthorhombic form solved by Golovina et al. [8] (See Table S1 in the supplementary Materials), indicating that they must consist of the same orthorhombic polymorph, whereas specimen “An” (right-hand panel in Figure 1) was identified by the authors as the monoclinic polymorph. It

is therefore likely that the differential thermal analysis (DTA) curve in the center panel in Figure 1 corresponds to the following process: melting of the orthorhombic form (peak c, onset 350 K or 77°C), recrystallization into the monoclinic form, which melts in turn (peak b in the center panel of Figure 1). An overview of this data can be found in Table 2, where for the sake of comparison and the calculations later on in the text all data have been provided in kelvin for the temperatures or in joule per gram for the enthalpy changes.

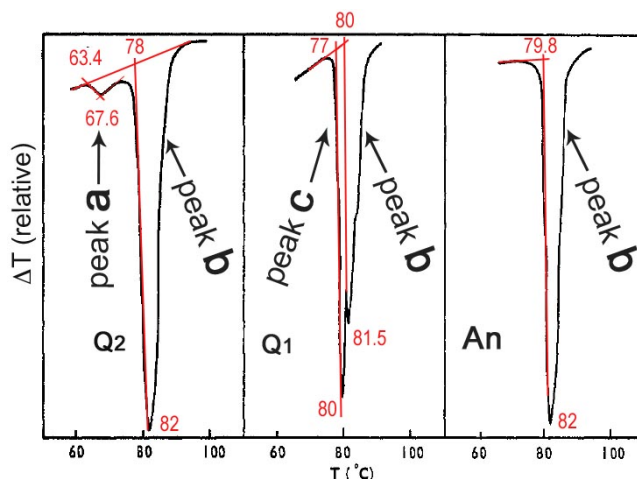


**Figure 1.** Differential thermal analysis curves of TNT modifications recorded at  $10 \text{ K min}^{-1}$  by Grabar et al. [18]. Specimens Q1 and Q2 correspond to the orthorhombic (O) modification (see Table T2) and specimen An is identified by the authors as being the monoclinic (M) polymorph. Peak **a** = O→M (onset at 336.6 K), peaks **c** + **b** = O→liquid→M→liquid, peak **b** = M→liquid (onset at 353 K). Figures from reference [18] and adapted for this paper.

Simultaneously, Connick et al. carried out calorimetric and crystallographic studies that revealed two kinds of thermal behavior (see Figure S1 in the supplementary materials) [19]. Single-peak DTA curves with an onset at about 354 K were ascribed to the melting of the monoclinic polymorph by the authors who observed that ‘single crystals grown from toluene solutions have a single peak melting endotherm and are monoclinic’. By contrast, ‘Double peaked endotherms are indicative of a mixture of the monoclinic and another polymorphic form, possibly orthorhombic. The proportion of each polymorph is variable and dependent on sample history’ according to the authors [19]. The melting of the orthorhombic form occurred in these measurements between 353 and 353.5 K (See Table 2).

Much later, in 1996, Gallagher et al, combining DSC, single-crystal and powder X-ray diffraction measurements found that the orthorhombic phase exhibits an endothermic transition into the monoclinic form at about 343 K on heating with an enthalpy of  $\Delta_{O \rightarrow M}H = 0.22 \text{ kcal mol}^{-1}$  ( $0.92 \text{ kJ mol}^{-1}$ ;  $4.05 \text{ J g}^{-1}$ ) [9]. The monoclinic form melted at about 351 or 352 K on further heating (see Figure S2 in the supplementary materials). Moreover, these authors reported that: “After an interval of two months all of the samples were reexamined and were found to be identical, and to yield powder pattern II [monoclinic]. This indicates that the solid associated with powder pattern I [orthorhombic] had undergone a structural transformation to the polymorphic form corresponding to material of powder pattern II during the intervening period” [9]. Nonetheless, no explicit storage conditions were provided by the authors. One year later, the same authors in a theoretical study concluded that the lattice energy of the monoclinic form is lower than that of the orthorhombic form [10]. In 2001 and 2003, Vrcelj et al. published DSC curves of the orthorhombic and monoclinic polymorphs [1, 2]. They have been reproduced in Figure S3 in the supplementary materials. It can be seen that a single melting endotherm is recorded on heating the monoclinic phase with an onset at 351-352 K (peak **b**), whereas on heating the orthorhombic phase, the melting peak of the monoclinic phase is preceded by another endothermic event with an onset at 340.6 K (peak **a**) ascribed to the orthorhombic to monoclinic transition. These authors also reported the related enthalpy change of this small event of 0.11

kcal mol<sup>-1</sup> (2.02 J g<sup>-1</sup>). The kinetics of the O→M transition were studied by Golovina et al. in 1994 and they observed this transition starting from a temperature of 55°C [8].

Other melting points of TNT have been reported in the literature. Chang et al. in 1987 found a value of 354.55K [17]. In 1990, Hwang et al. reported a melting point for TNT of 352 K (79 °C) with a melting enthalpy of  $\Delta_{\text{fus}}H = 5.8 \text{ kcal mol}^{-1}$  (24.27 kJ mol<sup>-1</sup>; 106.84 J g<sup>-1</sup>) [20]. The authors also determined the heat of vaporization  $\Delta_{\text{vap}}H = 19.5 \text{ kcal mol}^{-1}$  (81.59 kJ mol<sup>-1</sup>) at a boiling point of 202°C and a heat of sublimation of  $\Delta_{\text{sub}}H = 25.1 \text{ kcal mol}^{-1}$  (105.02 kJ mol<sup>-1</sup>; 462.36 J g<sup>-1</sup>) [20]. In the same year, Hu et al. found a melting point for TNT of  $T_{\text{fus}} = 80.6^\circ\text{C}$  (353.75 K) with a melting enthalpy of  $\Delta_{\text{fus}}H = 22.41 \text{ kJ mol}^{-1}$  (98.66 J g<sup>-1</sup>) [21]. In 2014, Kumar and Rao found a melting point of  $T_{\text{fus}} = 80.6^\circ\text{C}$  (353.75 K) and a melting enthalpy of  $\Delta_{\text{fus}}H = 25.1 \text{ kcal mol}^{-1}$  (22.36 kJ mol<sup>-1</sup>; 98.45 J g<sup>-1</sup>) [22]. In addition, they determined the heat capacity of TNT in the solid state from 17 to 67 °C leading to  $C_{p,\text{solid}}/\text{J g}^{-1} \text{ }^\circ\text{C}^{-1} = 1.063 + 3.14 \times 10^{-3} (T/^\circ\text{C})$  and that of the liquid state in the range from 97 to 150°C:  $C_{p,\text{liquid}}/\text{J g}^{-1} \text{ }^\circ\text{C}^{-1} = 1.293 + 1.46 \times 10^{-3} T/^\circ\text{C}$ , however, the authors did not specify the polymorph they used for the  $C_p$  measurements [22]. A glass transition of TNT was reported at a temperature of 258 K by May et al. in 1969 in addition to a melting enthalpy of 23.53 cal g<sup>-1</sup> (22.36 kJ mol<sup>-1</sup>; 98.45 J g<sup>-1</sup>) [23]. Shamim et al, used a flash DSC and found  $T_g$  values ranging from 239.3 to 247.5 K by heating the glass at rates from 10 to 1000 K s<sup>-1</sup> [24].

The vapor pressure of solid TNT was measured in the range from 327 K to 349 K by Lenchitz and Velicky, leading to the following expression [25]:

$$\text{Log} (P/\text{mmHg}) = -5400.536/(T/\text{K}) + 13.077 \quad (1a)$$

It results in a sublimation enthalpy for TNT of  $\Delta_{\text{sub}}H = 103.39 \text{ kJ mol}^{-1}$  (455.21 J g<sup>-1</sup>) with  $R = 8.31446 \text{ J mol}^{-1} \text{ K}^{-1}$ . Pella obtained the vapor pressure values of solid TNT in the 287-330 K range leading to the expression [26]:

$$\text{Ln} (P/\text{Pa}) = -11999/(T/\text{K}) + 33.513 \quad R^2 = 0.984 \quad (1b)$$

This leads to a sublimation enthalpy of  $\Delta_{\text{sub}}H = 99.765 \text{ kJ mol}^{-1}$  (439.24 J g<sup>-1</sup>). Finally, Cundall et al. determined the vapor pressure in the range of 301.4-346.1 K [27]:

$$\text{Log}_{10} (P/\text{N m}^{-2}) = -5900/(T/\text{K}) + 12.60 \quad (1c),$$

resulting in a  $\Delta_{\text{sub}}H = 113.0 \text{ kJ mol}^{-1}$  (497.3 J g<sup>-1</sup>).

The main calorimetric data mentioned here have been summarized in Table 2. From the data, it can be tentatively concluded that two polymorphs of TNT are confirmed: a monoclinic phase (form I), that melts at about  $352.9 \pm 1.3 \text{ K}$  and which tends to form heavily twinned crystals, and an orthorhombic phase, form II, that transforms endothermically to the monoclinic one and for which the lowest transformation has been observed at 328 K.

**Table 2. Available calorimetric data for TNT from the literature <sup>a</sup>**

$T_{O \rightarrow M}/\text{K}$	$\Delta_{O \rightarrow M}H/\text{J g}^{-1}$	$T_{S \rightarrow L}/\text{K}$	$\Delta_{S \rightarrow L}H/\text{J g}^{-1}$	$\Delta_{S \rightarrow v}H/\text{J g}^{-1}$	$\Delta_{L \rightarrow v}H/\text{J g}^{-1}$	Ref
336-337	4.93	351-353 (M) 350 (O)	-			[18]
		354 (M) 353-353.5 (O)				[19]

343	4.05	351-352 (M)				[9]
340.6	2.02	351-352 (M)				[1, 2]
328						[8]
		354.55				[17]
		352	106.84	462.36	360.57	[20]
		353.75	98.66			[21]
		353.75	98.45			[22]
			98.45			[23]
				455.21		[25]
				439.24		[26]
				497.3		[27]

<sup>a</sup> All data has been converted into kelvin for the transition temperatures and into joule per gram for the enthalpy changes to facilitate the calculations below in the text, M: monoclinic, O: orthorhombic

## 2.2 LIQUID DENSITY

Moore et al measured the density of liquid TNT as a function of temperature and found that “density was a linear function of temperature over a 20-40° range including 10-20° of supercooling”. They expressed dependence of the liquid density on the temperature with the following equation:  $\rho_L$  (g cm<sup>-3</sup>) =  $\rho_0 - \beta T/^\circ\text{C}$ , in which  $\rho_0$ , the liquid density at 0°C, and  $\beta$ , the thermal expansion, are 1.5450 g cm<sup>-3</sup> and 1.0244 × 10<sup>-3</sup> g cm<sup>-3</sup> K<sup>-1</sup>, respectively [28]. This dependence of the liquid (L) density on the temperature can be converted to the specific volume:

$$v_L/\text{cm}^3 \text{ g}^{-1} = 0.52170 + 0.0004596 T/\text{K} \quad (2)$$

The expansivity  $\alpha_{v,L}$  related to this expansion is 8.81 × 10<sup>-4</sup> K<sup>-1</sup>, which is near the value of 11.9 × 10<sup>-4</sup> K<sup>-1</sup>, found for the liquid expansivity of molecular compounds [12-14].

## 3 DATA ANALYSIS

### 3.1 THE SPECIFIC VOLUMES OF THE DIFFERENT PHASES

The values of specific volumes from Duke [9], from Golovina et al. [8], and from Vrcelj et al. [2] indicate that  $v_M < v_O$  at room temperature. It is significant that these three independent measurements come to the same conclusion even if the specific volumes of the two polymorphs are very close. Simply calculating the average of the difference, one obtains  $\Delta_{O \rightarrow MV} = -3.0 (\pm 2.4) \times 10^{-3} \text{ cm}^3 \text{ g}^{-1}$ . Nonetheless, if one uses the expansivities of the two phases together with their specific volume determined at low temperature by Vrcelj [2] and one determines the respective thermal expansion of the orthorhombic and the monoclinic form as a function of temperature, using  $v_{\text{phase}}/\text{cm}^3 \text{ g}^{-1} = v_0 + \alpha_{\text{phase}} v_0 T/\text{K}$  one finds for the orthorhombic form  $v_O = 0.57306 + 1.117 \times 10^{-4} T$  and for the monoclinic form  $v_M = 0.57208 + 1.167 \times 10^{-4} T$ . Using these equations to determine the specific volumes of the two forms at room temperature, the difference  $\Delta_{O \rightarrow MV}$  has become positive. Apparently, the expansivities are not accurate enough to be used for the determination of the difference in specific volume between the two polymorphs at room temperature. In particular because two of the direct

determinations of the specific volume clearly indicate that polymorph O has a slightly larger volume than polymorph M at room temperature. To correct for this, the average of the thermal expansivity for both forms is taken,  $1.995 \times 10^{-4} \text{ K}^{-1}$ , to calculate the two thermal expansions leading to the equations for the specific volume as a function of temperature in the following way:

$$v_0 = 0.57275 + 1.143 \times 10^{-4} T \quad (3)$$

$$v_M = 0.57233 + 1.142 \times 10^{-4} T \quad (4).$$

In this way the thermal expansion is reasonably well accounted for, while the specific volumes do not cross each other. Based on the available information in the literature, it can thus be concluded that the specific volume of the monoclinic form is (only slightly) smaller than that of the orthorhombic one, i.e.  $\Delta_{O \rightarrow MV} = v_M - v_0 < 0$ .

Another observation, which may be deceptive, is the paper by Stevens et al. on the behavior of TNT under pressure [4]. It is shown in the paper that when TNT is subjected to pressures above 23 GPa and in particular up to 35 GPa, it has turned into the orthorhombic form on returning to zero pressure [4]. Although, it is tempting to conclude that the orthorhombic phase forms under pressure, the observation in the paper is made at zero pressure. Therefore, it may be suggested that TNT has merely amorphized under pressure, as is not uncommon for organic substances [29, 30], and when returning back to zero pressure, it has recrystallized into one of its available polymorphs. In that respect, Vrcelj already states that both the monoclinic and orthorhombic structures are closely related, so that slight amorphization may distort the structure enough to cause it to recrystallize in the different form [1, 2]. Taking into consideration that three independent X-ray diffraction measurements indicate that the monoclinic form is the densest form of the two polymorphs [2, 8, 9], the pathway of formation of the orthorhombic form under ambient pressure after amorphization of the monoclinic form under pressure seems the most likely, in particular, because it is thermodynamically impossible that a system spontaneously expands, while a pressure is being applied.

### 3.2 THE ENTHALPY CHANGES OF THE DIFFERENT PHASE TRANSITIONS

The four enthalpies of fusion in Table 2 which can be ascribed to the melting of the monoclinic form, lead to a mean value of  $100.6 \pm 4.2 \text{ J g}^{-1}$ . Four values for the heat of sublimation have been found in the literature (Table 1). Their mean value equals  $463 \pm 25 \text{ J g}^{-1}$ . Hwang et al. also determined the enthalpy of vaporization with a value of  $360.57 \text{ J g}^{-1}$ . The difference between the two vapor pressure enthalpies should again be equal to the heat of fusion,  $\Delta_{M \rightarrow LH} = \Delta_{M \rightarrow VH} - \Delta_{L \rightarrow VH}$  (with V: vapor phase) and leads to  $103 \text{ J g}^{-1}$ , very similar to the mean value of the direct measurements, which confirms the vapor pressure enthalpies.

The orthorhombic-to-monoclinic phase transition (peak 'a' in Figure 1 [18] and in Figures S2 [9] and S3 [1, 2]) is endothermic in all the different papers demonstrating that heating favors the equilibrium to shift to the monoclinic polymorph. This proves that the two polymorphs have an enantiotropic phase relationship and that, in accordance with the Le Chatelier principle, the orthorhombic form must be stable somewhere at low temperature. This assessment is in conflict with the conclusions drawn in previous papers [1-3]. However, the value of the enthalpy change associated with the transition is less clear, because the three observed values range from 2 to  $4.9 \text{ J g}^{-1}$  (Table 1). To verify the enthalpies, the areas of peaks 'a' and 'b' in Figure 1 and in Figures S2 and S3 in the supplementary materials have been remeasured using the peak delimitation as defined in Figure S5 in the supplementary materials. The enthalpy change related to peak 'a' was determined assuming that the area of peak 'b' corresponds to  $\Delta_{M \rightarrow LH} = 100.6 \text{ J g}^{-1}$ . Whereas  $\Delta_{O \rightarrow MH}$  values of about  $5 \text{ J g}^{-1}$  were found with the 'a' peaks from Figure 1 [18] and Figure S2 [9] agreeing with the results published by these authors (see Table 1), a value as high as  $11 \text{ J g}^{-1}$  was found for peak 'a' in Figure S3 and it disagrees with the value of  $2.02 \text{ J g}^{-1}$  reported by the authors [1, 2]. Therefore discarding the latter reported value, the mean transition enthalpy has been determined based on the values from references [9, 18] resulting in a value of  $\Delta_{O \rightarrow MH} = 4.5 \text{ J g}^{-1}$ .



Solid-solid transition temperatures are known to be delayed and may be observed at a higher temperature, when measured by DSC, than the real equilibrium temperature [31-33]. In the available literature, the lowest temperature for the observation of the O→M transition has been reported by Golovina et al. at 328 K (Table 1)[8]. Related to the position of the solid-solid equilibrium, is the question where the melting point of form O can be found. In this respect, it is clear that the melting point of form O cannot be positioned at a lower temperature than where the O→M transitions have been observed, otherwise O would have molten instead of transformed into M. It being clear from the literature that form M is the highest melting form, the melting equilibrium of form O must be found between the melting point of M and the observations of the O→M transition in the solid. This brings us to Figure S1 in the supplementary materials, which indicates that form O melts about one degree lower than form M [19]. Taking this temperature difference and applying that to the average melting temperature determined for form M of  $352.9 \pm 1.3$  K, form O would be expected to melt at 352 K. The melting points can be used to determine the solid-solid transition temperature using eq. 5 [34]:

$$T_{O \rightarrow M} = \frac{\Delta_{M \rightarrow L}H - \Delta_{O \rightarrow L}H}{\frac{\Delta_{M \rightarrow L}H}{T_{M \rightarrow L}} - \frac{\Delta_{O \rightarrow L}H}{T_{O \rightarrow L}}} = \frac{\Delta_{M \rightarrow L}H - \Delta_{O \rightarrow L}H}{\Delta_{M \rightarrow L}S - \Delta_{O \rightarrow L}S} \approx \frac{\Delta_{O \rightarrow M}H}{\Delta_{O \rightarrow M}S} \quad (5)$$

The melting enthalpy of the orthorhombic phase can be found by adding the difference in enthalpy between the two solid phases  $\Delta_{O \rightarrow L}H = \Delta_{M \rightarrow L}H + \Delta_{O \rightarrow M}H = 105.1$  J g<sup>-1</sup>. Then with the melting points found just above, one finds for the transition point 330.9 K, which confirms the transition temperature observed by Golovina of 328 K [8]. Thus, as is clear from the literature, the orthorhombic form can either transform to the monoclinic one through a solid-to-solid endothermic transition, melt, or melt and convert into the monoclinic form on heating as illustrated in Figure S1 in the supplementary materials [19]. Similar thermal behavior has been observed previously with piracetam phase III that either transforms to phase I or melts without transformation depending on the presence of traces of residual solvent [33, 35].

### 3.3 CONSTRUCTION OF THE PRESSURE-TEMPERATURE TOPOLOGICAL PHASE DIAGRAM

The construction of pressure-temperature phase diagrams through the Clapeyron equation has been described previously [14, 36, 37]. The Clapeyron equation:

$$\frac{dP}{dT} = \frac{\Delta H}{T\Delta V} \quad (6),$$

can be used to calculate the slopes of the two-phase equilibrium curves using the enthalpy and volume changes of the related phase transitions. In particular solid-solid phase equilibria are straight lines over extensive temperature and pressure ranges [38]; therefore, the slope can be used to describe such a phase transition with a straight line.

### 3.4 PRESSURE-TEMPERATURE MELTING CURVES FOR THE TWO POLYMORPHS

Summarizing the conclusions of the foregoing paragraphs, the temperatures and the heats of fusion of the two polymorphs are:  $T_{M \rightarrow L} = 352.9$  K,  $\Delta_{M \rightarrow L}H = 100.6$  J g<sup>-1</sup> and  $T_{O \rightarrow L} = 351.9$  K, and  $\Delta_{O \rightarrow L}H = 105.1$  J g<sup>-1</sup>. At the melting point of the monoclinic form, the specific volumes of the solid and the liquid can be calculated using eqs. 4 and 2:  $v_M(352.9 \text{ K}) = 0.612625$  cm<sup>3</sup> g<sup>-1</sup> and  $v_L(352.9 \text{ K}) = 0.683896$  cm<sup>3</sup> g<sup>-1</sup> leading to a change in volume on melting of  $\Delta_{M \rightarrow L}V = 0.071271$  cm<sup>3</sup> g<sup>-1</sup>. In the case of the orthorhombic solid, eqs. 3 and 2 lead to:  $v_O(351.9 \text{ K}) = 0.612955$  cm<sup>3</sup> g<sup>-1</sup>,  $v_L(351.9 \text{ K}) = 0.683436$  cm<sup>3</sup> g<sup>-1</sup>, and  $\Delta_{O \rightarrow L}V = 0.070482$  cm<sup>3</sup> g<sup>-1</sup>. These values can be used to evaluate the slopes of the two melting equilibria with the Clapeyron equation, leading to  $dP/dT_{M \rightarrow L} = 4.00$  MPa K<sup>-1</sup> and  $dP/dT_{O \rightarrow L} = 4.24$  MPa K<sup>-1</sup>.

Using the slopes, the pressure-temperature melting curves can be obtained by approximating them by straight lines. The melting point of the respective polymorphs can be considered a triple point, because the vapor pressure of the condensed phases around the melting temperature is in the order of 0.68 Pa, obtained with the equation reported by Pella [26] at 353 K. Such a pressure can be safely neglected by using 0 MPa for the pressure of the respective triple points with temperatures equivalent to the melting points. Using expressions of the form  $P_{M \rightarrow L}/\text{MPa} = 4.00 T/\text{K} + B_{M \rightarrow L}$ , the constants are found to be:  $B_{M \rightarrow L} = -1411.5$  and  $B_{O \rightarrow L} = -1491.0$ . This results in the following equations for the melting curves with pressure in MPa and temperature in K:

$$P_{M \rightarrow L} = 4.00 T - 1411.5 \quad (7)$$

$$P_{O \rightarrow L} = 4.24 T - 1491.0 \quad (8)$$

With these two melting curves the triple point O-M-L, their intersection, can be determined and its coordinates can be calculated by setting eqs. 7 and 8 equal to each other:  $T_{O-M-L} = 335$  K and  $P_{O-M-L} = -71$  MPa.

### 3.5 THE PRESSURE-TEMPERATURE EQUILIBRIUM CURVE BETWEEN THE TWO SOLIDS

Solid-solid equilibria in a P-T diagram are usually found to be straight lines [38-40]. The O-M equilibrium curve passes through the O-M-vapor triple point, whose coordinates are 330.9 K and 0 MPa, and the O-M-L triple point, whose coordinates can be found just above. With these two sets of coordinates, the equation of the O-M equilibrium curve is found to be (P/MPa, T/K):

$$P_{O-M} = -17.2 T + 5690 \quad (9)$$

The slope of the O-M equilibrium can also be calculated with the Clapeyron equation using the data at its transition temperature calculated above:  $T_{O \rightarrow M} = 330.9$  K,  $\Delta_{O \rightarrow M}H = 4.5$  J g<sup>-1</sup>,  $\Delta_{O \rightarrow M}V = -4.42 \times 10^{-4}$  cm<sup>3</sup> g<sup>-1</sup>. In that case one obtains  $P_{O-M} = -30.7 T + 10159$ , a line that is even steeper. One has to realize that in this respect  $-17.2$  or  $-30.7$  only indicates that the slope of the equilibrium line is negative and very steep; the actual value of the slope is of very little importance. It can be seen that the dP/dT slope of the O-M equilibrium line is far greater than those of the melting curves and is due to the minute difference between the specific volumes of the polymorphs. The O-M transition is therefore mainly entropy driven and that also implies that increasing the pressure will have very little effect in transforming the stability conditions between the polymorphs. In fact, at room temperature, where the orthorhombic form is stable, following eq. 9, the monoclinic form would only become stable above  $-17.2 \times 298 + 5690 = 564$  MPa. This would in principle still be in contradiction with the observation of Stevens et al. [4] of the formation of the orthorhombic polymorph at or below a pressure of 34 GPa; however, because the observation was carried out under atmospheric pressure, the pressure range from 564 to 0 MPa, would leave the system with a considerable pressure window to crystallize in the orthorhombic system either from the amorphous state or even from the monoclinic form damaged by the pressure.

### 3.6 EQUILIBRIA INVOLVING THE VAPOR PHASE

When vapor (V) is produced in the presence of condensed phases, phase changes between the condensed phases will approximate triple points. For TNT, this would be the case for transitions M→L, O→L, and O→M, whose temperatures are those of triple points M-L-V, O-L-V, and O-M-V, respectively.

Because sublimation and vaporization curves are usually described by Clausius-Clapeyron type equations:  $\ln(P_V) = -\Delta_v H/(RT) + B$ , in which  $P_V$  is the vapor pressure and  $\Delta_v H$  is the enthalpy change of either sublimation or vaporization. All two-phase equilibria of TNT involving the vapor phase can be obtained through eqs. 1a, 1b, or 1c. Other necessary data is the enthalpy change for the solid-solid transition or for both melting transitions. It should be realized that the vapor pressures of two condensed phases in equilibrium are equal and due to the fact that enthalpy is a state function, its algebraic sum of a change cycling around a triple point and returning to the initial state will equal 0.

If eq. 1b is used for the sublimation of the orthorhombic form,  $\Delta_{L \rightarrow V}H = \Delta_{O \rightarrow V}H - \Delta_{O \rightarrow L}H = 439.24 - 105.09 = 334.15 \text{ J g}^{-1} = 75896 \text{ J mol}^{-1}$ . The vapor pressures of O and L are equal at the triple temperature  $T_{O-L-V}$  and therefore using eq. 1b, one gets:  $\ln(P_O) = 33.513 - 11999/T = \ln(P_L) = B_L - 9128/T$ . With  $T_{O \rightarrow L} = 351.9 \text{ K}$  and  $R = 8.3145 \text{ J mol}^{-1} \text{ K}^{-1}$ , constant  $B_L$  is found to be 25.35 and for  $\ln(P_L/\text{Pa})$ , this leads to:

$$\ln(P_L) = 25.35 - 9128/T \text{ with } T \text{ in K} \quad (10)$$

Using equation (10), the sublimation curve for the M-phase melting at 352.9 K can be found following the same procedure:  $\Delta_{M \rightarrow V}H = \Delta_{L \rightarrow V}H + \Delta_{M \rightarrow L}H = 334.15 + 100.6 = 434.75 \text{ J g}^{-1} = 98745 \text{ J mol}^{-1}$ . At triple point M-L-V, the vapor pressures  $P_L$  and  $P_M$  are equal and therefore,  $\ln P_L = 25.35 - 9128/T = \ln P_M = B_M - 11876/T$ , which leads to  $B_M = 33.14$  and

$$\ln(P_M) = 33.14 - 11876.19/T \text{ with } P_M \text{ in Pa and } T \text{ in K} \quad (11)$$

With eqs. 1b and 11, the vapor pressures of phases O and M can be compared at room temperature (298 K). It can be seen that  $P_O(298 \text{ K}) = 1.17 \times 10^{-3} \text{ Pa}$  is smaller than  $P_M(298 \text{ K}) = 1.22 \times 10^{-3} \text{ Pa}$ . The difference reflects the thermodynamic stability ranking with the more stable phase possessing a smaller vapor pressure.

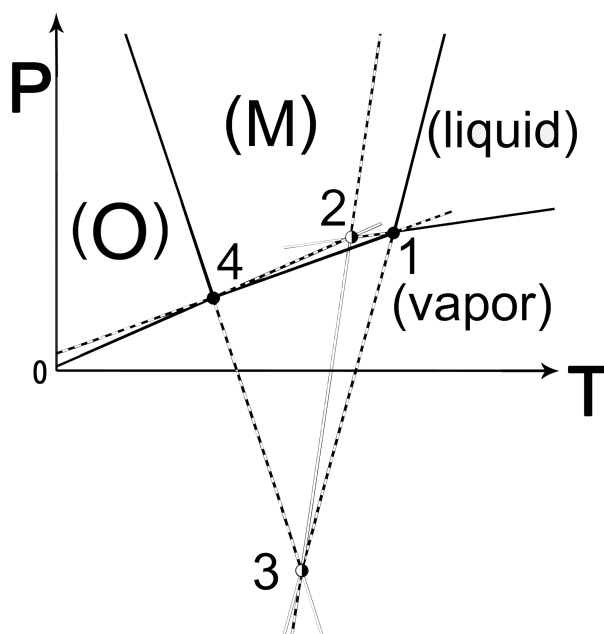


**Figure 2.** Topological pressure-temperature phase diagram of TNT representing the stability regions of forms O and M, the liquid (L) and the vapor (V) phase. Triple points: 1: M-L-V, 2: O-L-V, 3: O-M-L, 4: O-M-V. Stability ranking: solid black lines: stable, dashed lines: metastable, white lines: supermetastable

## 4 CONCLUDING REMARKS

The topological pressure-temperature diagram for the dimorphism of TNT, constructed using data available from the literature, is found to be a case of overall enantiotropic behavior corresponding to Bakhuis-Roozeboom's case 2 [41-43].

It has been demonstrated in this article in accordance with observation [1, 2, 8, 9, 18] that the orthorhombic form endothermically transforms to the monoclinic form at about 331 K on heating. Although the temperature of a solid-solid equilibrium remains difficult to determine [32], considering the reported data and the outcome of the topological phase diagram, the orthorhombic form is most likely the stable form at room temperature. The spontaneous transformation of the orthorhombic form into the monoclinic form observed in samples left for two months [9] appears difficult to explain; however, storage conditions were

not clearly defined in the paper and samples could have been subjected to temperature fluctuations. In addition, impurities could have been present, which is known to affect the stability behavior of chemical substances due to the formation of solid solutions.

The accuracy of the topological phase diagram improves if the dependence of the specific volumes on the temperature is known, as is the case for the data on TNT. The specific volume of crystalline molecular solids can nowadays be determined over a large temperature interval of 100 to 473 K thanks to the coupling of X-ray diffractometry and commercially available devices for temperature control. Nonetheless, this is not the case for the specific volumes of molecular compounds in the molten state, because such compounds decompose while melted and because the available methods are seldomly employed.

In previous papers, the volume change on melting for a number of molecular compounds has been reported at their respective temperatures of fusion. Interestingly, the ratio  $v_{\text{liquid}}/v_{\text{solid}}$  on melting is rather constant and equals  $1.11 \pm 0.04$  [12, 13, 44]. TNT confirms this ratio, as using eqs. (2) and (4), leads to  $v_{\text{liquid}}/v_{\text{solid}} = 1.116$ , thus reinforcing the predictive character of this statistical value. However, in the case that multiple polymorphs exist, the ratio should be applied to the highest melting polymorph. Therefore, the dependence of the specific volume of the liquid should be known if the volume change on melting of other polymorphs is required for the calculation of the  $dP/dT$  slopes of the melting curves with the Clapeyron equation. Statistical analysis has shown that the expansivity of molecular liquids possesses an average value of  $1.19 \cdot 10^{-3} \text{ K}^{-1}$  [12, 13, 44]. For TNT, an experimental value of about  $0.9 \cdot 10^{-3} \text{ K}^{-1}$  has been found, which is on the small side, but still near the average value.

Finally, another important ratio for the determination of topological phase diagrams is the  $v_{\text{liquid}}/v_{\text{solid}}$  ratio between the metastable liquid and the crystalline phase at the temperature of the glass transition. For TNT, whose glass transition temperature was found ranging from 239 to 258 K, the ratio lies between 1.052 and 1.063 depending on the  $T_g$  value used in eqs. 2 and 3. Unfortunately, not enough data exists so far to judge its statistical importance.

### **Competing Interests**

No competing interests to declare

### **Supplementary Materials**

Table comparing experimental X-ray patterns, several annotated DSC curves.

## Supplementary Material

**Table S1.** Comparison of the X-ray diffraction pattern of specimen Q used by Grabar et al. [18] with the pattern calculated from the crystal structure of the orthorhombic polymorph solved by Golovina et al. (ZZZMUC05 [8]).

Grabar (exp)		Golovina (calc)	
$d_{hkl}$	$I/I_1$	$d_{hkl}$	$I/I_0$ (%)
10.2	20	10.02	1.5
7.08	50	7.03	40
6.02	10	6.008	3
5.71	40	5.638	35
5.43	40	5.428	26
5.01	40	5.000	21
4.77	10	4.720	2
4.31	60	4.304	16
		4.264	25
3.88	100	3.862	100
3.72	30	3.741	14.5
		3.688	12
3.56	20	3.530	11
3.45	20	3.433	14
3.28	40	3.260	36
3.16	10	3.150	5
3.05	50	3.050	11
		2.992	25
2.89	40	2.875	24

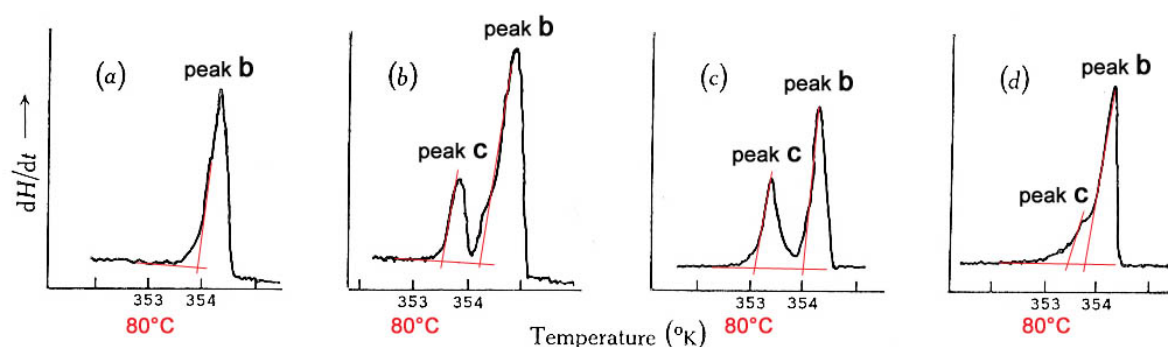
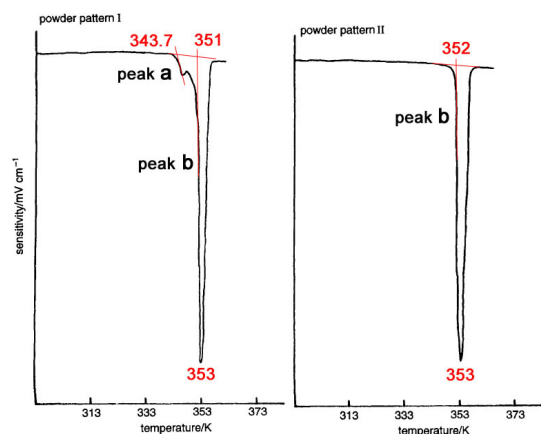
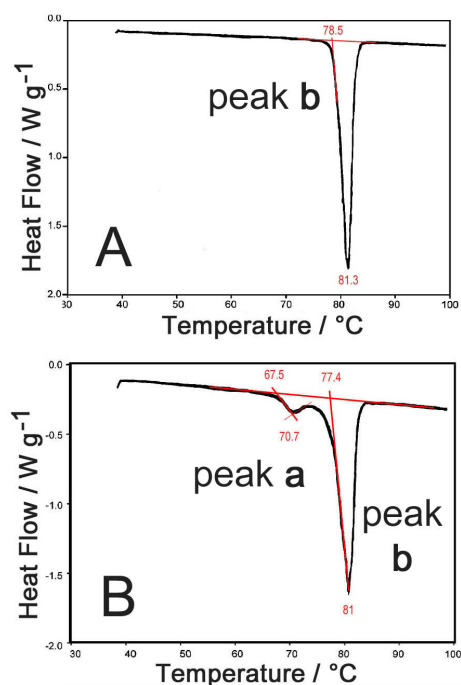


Fig. 1.—Endotherms. (a) Recrystallized TNT; (b) recrystallized, melted; (c) sublimed; (d) sublimed, melted.

**Figure S1.** Differential thermal analysis curves for TNT reported by Connick et al. [19]. It was observed that monoclinic single crystals recrystallized from toluene solutions exhibited a single melting peak (peak 'b', panel a). However, convoluted peaks were observed in the case of mixtures of polymorphs (monoclinic and most likely the orthorhombic one) in various ratios (panels b – d). Thus peak 'c' is most likely the melting of the orthorhombic polymorph occurring at about one degree lower than the monoclinic one.



**Figure S2.** DSC curves by Gallagher et al. for the orthorhombic (left-hand panel) and monoclinic (right-hand panel) polymorphs of 2,4,6-trinitrotoluene [9].



**Figure S3.** DSC curves of TNT published by Vrcelj et al. [1, 2]: panel A monoclinic form (M) and panel B orthorhombic form (O). Peak 'a' = O→M (onset at 340.6 K), peak 'b' = M→liquid (onset at 351-352 K).

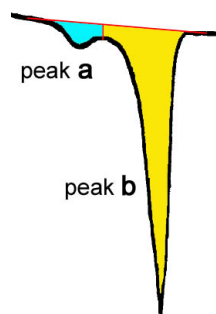


**Figure S4.** Delimitation of peaks 'a' and 'b' for Figure 1 in the text and Figures S2 and S3 in the supplementary materials. The yellow area is ascribed to the heat of fusion of the monoclinic polymorph and the blue area to the transition of form O into form M.

## REFERENCES

1. Vrcelj RM, Gallagher HG, Sherwood JN. Polymorphism in 2,4,6-trinitrotoluene crystallized from solution. *J Am Chem Soc.* 2001;123(10):2291-5. doi:DOI 10.1021/ja0031422.
2. Vrcelj RM, Sherwood JN, Kennedy AR, Gallagher HG, Gelbrich T. Polymorphism in 2-4-6 trinitrotoluene. *Cryst Growth Des.* 2003;3(6):1027-32. doi:10.1021/cg0340704.
3. Bowden PR, Chellappa RS, Dattelbaum DM, Manner VW, Mack NH, Liu Z. The high-pressure phase stability of 2,4,6-trinitrotoluene (TNT). *Journal of Physics: Conference Series.* 2014;500:052006. doi:10.1088/1742-6596/500/5/052006.
4. Stevens LL, Velisavljevic N, Hooks DE, Dattelbaum DM. The high-pressure phase behavior and compressibility of 2,4,6-trinitrotoluene. *Appl Phys Lett.* 2008;93(8):081912. doi:10.1063/1.2973162.
5. Hultgren R. An X-ray study of symmetrical trinitrotoluene and cyclo trimethylenetrinitramine. *J Chem Phys.* 1936;4:84. doi:10.1063/1.1749756.
6. Winchell AN. *The optical properties of organic compounds.* 2nd edition ed. New York: Academic Press; 1954.
7. Carper WR, Davis LP, Extine MW. Molecular-Structure of 2,4,6-Trinitrotoluene. *J Phys Chem.* 1982;86(4):459-62. doi:DOI 10.1021/j100393a009.
8. Golovina NI, Titkov AN, Raevskii AV, Atovmyan LO. Kinetics and Mechanism of Phase-Transitions in the Crystals of 2,4,6-Trinitrotoluene and Benzotrifuroxane. *J Solid State Chem.* 1994;113(2):229-38. doi:DOI 10.1006/jssc.1994.1365.
9. Gallagher HG, Sherwood JN. Polymorphism, twinning and morphology of crystals of 2,4,6-trinitrotoluene grown from solution. *J Chem Soc Faraday Trans.* 1996;92(12):2107-16. doi:DOI 10.1039/ft9969202107.
10. Gallagher HG, Roberts KJ, Sherwood JN, Smith LA. A theoretical examination of the molecular packing, intermolecular bonding and crystal morphology of 2,4,6-trinitrotoluene in relation to polymorphic structural stability. *J Mater Chem.* 1997;7(2):229-35. doi:DOI 10.1039/a603983i.
11. Gallagher HG, Vrcelj RM, Sherwood JN. The crystal growth and perfection of 2,4,6-trinitrotoluene. *J Cryst Growth.* 2003;250(3-4):486-98. doi:10.1016/S0022-0248(02)02394-1.
12. Céolin R, Rietveld IB. The topological pressure-temperature phase diagram of ritonavir, an extraordinary case of crystalline dimorphism. *Ann Pharm Fr.* 2015;73(1):22-30. doi:10.1016/j.pharma.2014.09.003.
13. Rietveld IB, Céolin R. Phenomenology of crystalline polymorphism: overall monotropic behavior of the cardiotonic agent FK664 forms A and B. *J Therm Anal Calorim.* 2015;120(2):1079-87. doi:10.1007/s10973-014-4366-2.
14. Céolin R, Rietveld IB. The topological phase diagram of cimetidine: A case of overall monotropy. *Ann Pharm Fr.* 2017;75:89-94.
15. Golder GA, Zhdanov GS, Umanskii MM, Glushkova VP. *Zh Fiz Khim.* 1952;26:1259.
16. Hertel E, Romer GH. *ZPhysChem(Leipzig).* 1930;B11:77.
17. Chang H-C, Tang C-P, Chen Y-J, Chang C-L. *Int Annual Conf Fraunhofer ICT.* 1987;18:51.
18. Grabar DG, Rauch FC, Fanelli AJ. Observation of a Solid-Solid Polymorphic Transformation in 2,4,6-Trinitrotoluene. *J Phys Chem.* 1969;73(10):3514-&. doi:DOI 10.1021/j100844a073.
19. Connick W, May FGJ, Thorpe BW. Polymorphism in 2,4,6-Trinitrotoluene. *Aust J Chem.* 1969;22(12):2685-&. doi:Doi 10.1071/Ch9692685.
20. Hwang D-R, Tamura M, Yoshida T, Tanaka N, Hosoya F. Estimation of  $\Delta H^{\circ}$  of nitro derivatives of benzene and toluene using AM1 and DSC. *Journal of Energetic Materials.* 1990;8(1-2):85-98. doi:10.1080/07370659008017247.
21. Hu RZ, Li JM, Liang YJ, Wu SX, Sun LX, Wang YP. Thermal-Behavior on 2,2,2-Trinitroethyl-4,4,4-Trinitrobutyrate. *J Therm Anal.* 1990;36(3):1155-60.
22. Kumar AS, Rao VD. Modeling of Cooling and Solidification of TNT based Cast High Explosive Charges. *Defence Sci J.* 2014;64(4):339-43.
23. May FGJ, Thorpe BW, Connick W. A glass transition in trinitrotoluene. *J Cryst Growth.* 1969;5:312.
24. Shamim N, Koh YP, Simon SL, McKenna GB. The glass transition of trinitrotoluene (TNT) by flash DSC. *Thermochim Acta.* 2015;620:36-9. doi:10.1016/j.tca.2015.10.003.
25. Lenchitz C, Velicky RW. Vapor Pressure and Heat of Sublimation of 3 Nitrotoluenes. *J Chem Eng Data.* 1970;15(3):401-&. doi:DOI 10.1021/je60046a022.
26. Pella PA. Measurement of Vapor-Pressures of TNT, 2,4-DNT, 2,6-DNT, and EGDN. *J Chem Thermodyn.* 1977;9(4):301-5. doi:Doi 10.1016/0021-9614(77)90049-0.
27. Cundall RB, Palmer TF, Wood CEC. Vapor-Pressure Measurements on Some Organic High Explosives. *J Chem Soc Farad T 1.* 1978;74:1339-45. doi:DOI 10.1039/f19787401339.

28. Moore DW, Burkardt LA, Mcewan WS. Viscosity and Density of the Liquid System Tnt-Picric Acid and 4 Related Pure Materials. *J Chem Phys.* 1956;25(6):1235-41. doi:Doi 10.1063/1.1743185.
29. Hedoux A, Guinet Y, Capet F, Paccou L, Descamps M. Evidence for a high-density amorphous form in indomethacin from Raman scattering investigations. *Phys Rev B: Condens Matter.* 2008;77(9):094205/1 - /10. doi:10.1103/PhysRevB.77.094205.
30. Hedoux A, Guinet Y, Derollez P, Willart JF, Capet F, Descamps M. Pressure-induced transformations and high-pressure behaviour in cyanoadamantane plastic crystal. *J Phys: Condens Matter.* 2003;15(49):8647-61. doi:10.1103/PhysRevB.77.094205.
31. Rietveld IB, Barrio M, Tamarit J-L, Nicolai B, Van de Streek J, Mahé N et al. Dimorphism of the Prodrug L-Tyrosine Ethyl Ester: Pressure-Temperature State Diagram and Crystal Structure of Phase II. *J Pharm Sci.* 2011;100(11):4774-82. doi:10.1002/jps.22672.
32. Barrio M, Maccaroni E, Rietveld IB, Malpezzi L, Masciocchi N, Ceolin R et al. Pressure-temperature state diagram for the phase relationships between benfluorex hydrochloride forms I and II: a case of enantiotropic behavior. *J Pharm Sci.* 2012;101(3):1073-8. doi:10.1002/jps.22821.
33. Toscani S, Céolin R, Ter Minassian L, Barrio M, Veglio N, Tamarit J-L et al. Stability hierarchy between piracetam forms I, II, and III from experimental pressure-temperature diagrams and topological inferences. *Int J Pharm.* 2016;497(1-2):96-105. doi:10.1016/j.ijpharm.2015.11.036.
34. Yu L. Inferring Thermodynamic Stability Relationship of Polymorphs from Melting Data. *J Pharm Sci.* 1995;84(8):966-74. doi:10.1002/Jps.2600840812.
35. Céolin R, Agafonov V, Louër D, Dzyabchenko VA, Toscani S, Cense JM. Phenomenology of Polymorphism, III:p,TDiagram and Stability of Piracetam Polymorphs. *J Solid State Chem.* 1996;122(1):186-94. doi:10.1006/jssc.1996.0100.
36. Céolin R, Rietveld IB. Phenomenology of polymorphism and topological pressure-temperature diagrams. *J Therm Anal Calorim.* 2010;102(1):357-60. doi:Doi 10.1007/S10973-010-0856-Z.
37. Ceolin R, Rietveld I. The topological pressure-temperature phase diagram of fluoxetine nitrate: monotropy unexpectedly turning into enantiotropy. *Eur Phys J - ST.* 2017;226:881-8. doi:10.1140/epjst/e2016-60275-1.
38. Ceolin R, Toscani S, Rietveld IB, Barrio M, Tamarit J-L. Pitfalls and feedback when constructing topological pressure-temperature phase diagrams. *Eur Phys J - ST.* 2017;226(5):1031-40. doi:10.1140/epjst/e2016-60246-6.
39. Gana I, Barrio M, Ghaddar C, Nicolai B, Do B, Tamarit J-L et al. An Integrated View of the Influence of Temperature, Pressure, and Humidity on the Stability of Trimorphic Cysteamine Hydrochloride. *Mol Pharmaceut.* 2015;12(7):2276-88. doi:10.1021/mp500830n.
40. Gana I, Barrio M, Do B, Tamarit J-L, Céolin R, Rietveld IB. Benzocaine polymorphism: Pressure-temperature phase diagram involving forms II and III. *Int J Pharm.* 2013;456(2):480-8. doi:10.1016/j.ijpharm.2013.08.031.
41. Bakhuis Roozeboom HW. Die heterogenen Gleichgewichte vom Standpunkte der Phasenlehre. Erstes Heft: Die Phasenlehre - Systeme aus einer Komponente. Braunschweig: Friedrich Vieweg und Sohn; 1901.
42. Ceolin R, Tamarit JL, Barrio M, Lopez DO, Nicolai B, Veglio N et al. Overall monotropic behavior of a metastable phase of biclotymol, 2,2'-methylenebis(4-chloro-3-methyl-isopropylphenol), inferred from experimental and topological construction of the related P-T state diagram. *J Pharm Sci.* 2008;97(9):3927-41. doi:10.1002/jps.21285.
43. Ceolin R, Rietveld I-B. X-ray crystallography, an essential tool for the determination of thermodynamic relationships between crystalline polymorphs. *Ann Pharm Fr.* 2016;74(1):12-20. doi:10.1016/j.pharma.2015.10.004.
44. Ceolin R, Rietveld IB. The topological phase diagram of cimetidine: A case of overall monotropy. *Ann Pharm Fr.* 2017;75(2):89-94. doi:10.1016/j.pharma.2016.11.002.